Ribo-attenuators: novel elements for reliable and modular riboswitch engineering

Thomas Folliard*[+], Thomas P Prescott[+], Christopher W Jones[+], Travis Bayer, Judith P Armitage[+], Antonis Papachristodoulou[+] & Lynn J Rothschild[&]*

+ University of Oxford, department of Biochemistry, South Parks Road, Oxford.

& National aeronautic and Space Administration Ames MOFFETT FIELD, CA 94035, USA

To whom correspondence should be addressed: Lynn.J.Rothschild@nasa.gov or Tom@folliard.org

Abstract

Riboswitches are structural genetic regulatory elements that directly couple the sensing of small molecules to gene expression. They have considerable potential for applications throughout synthetic biology and bio-manufacturing as they are able to sense a wide range of small molecules and in response regulate gene expression. Despite over a decade of research they have yet to reach this considerable potential as they cannot be treated as modular components. This is due to several limitations including, sensitivity to changes in genetic context, low tunability and large degrees of variation.

To overcome the associated difficulties with riboswitches, we have designed and introduced a novel genetic element called a Ribo-attenuator. This genetic element allows for predictable tuning, insulation from contextual changes and a reduction in expression variation. Ribo-attenuators allow riboswitches to be treated as a truly modular and tunable component, and thus increase their reliability for a wide range of applications.

Introduction

Riboswitches are structural regulatory elements mostly present in the 5' UTR of messenger RNA, found in all three domains of life [1]. Relying solely on RNA for structure, it is possible that they originated as a very early regulatory element in a hypothesized RNA world [2].They usually allow the regulation of a downstream gene or operon in response to the binding of small molecules such as cellular metabolites or metal ions [3–6]. Some regulate transcription or translation while others regulate splicing in eukaryotes[7]. Riboswitches that regulate translation do so through the allosteric effects of small molecules binding to their aptamer domain. This structural rearrangement usually opens up or sequesters away a ribosome binding site (RBS) core (figure 1) [8–10]. While many riboswitches evolved to control the expression of enzymes in natural systems, synthetic riboswitches have been adapted from natural ones to respond to specific molecules [11–16]. These studies along with recent advances towards the *in silico* design of riboswitches [17–19] represent significant scientific interest in the application of riboswitches.

Despite significant promise and over a decade of research, limitations inherent in riboswitch function reduce their applicability. Many riboswitches rely on a specific secondary structure to selectively bind the small molecule of interest. This secondary structure often results not just from within their aptamer domain, but also the proximal open reading frame (ORF) that the riboswitch controls the expression of. Changing the ORF to suit another application can destroy any response of the riboswitch to the small molecule it usually responds to [20]. Ideally, riboswitches could be treated as modular "plug and play" devices compatible with a library of ORFs allowing for the construction of genetic networks responding to small molecules. Many studies claiming modularity of riboswitches employ a fusion comprised of a riboswitch, the first few hundred base pairs of its working ORF and a gene of interest. However, this fusion can affect functionality of a gene, as many enzymes will not function with 5' fusions, limiting their translation from riboswitches [21–26]. This use of fusions demonstrates the inherent sensitive nature of riboswitches and is subsequently a barrier to the generation of truly modular riboswitches.

A further limitation is the difficulty in altering the functional range in response to a ligand. The induction or repression response comes not only from the riboswitch RBS strength but also from their secondary structure[19]. Changing this induction response to suit a novel application remains a major hurdle not yet explored. Typically, changing an RBS can lead to a different activation range of a conventional transcription factor bases biosensor. However, due to the specificity of secondary structure surrounding the aptamer domain of riboswitch and a poor understanding of *in vivo* RNA structures, changing the riboswitch induction range without destroying the induction response is difficult. Despite advances towards the *in silico* design of riboswitches [19], inducers are limited and the dynamic range cannot be easily and predictably changed.

A further limitation to some synthetic or re-engineered riboswitches is variation in downstream gene expression. This noise in riboswitch function is thought to originate from ligand dependent RBS accessibility bursts [8] and is a major limitation in many high throughput screening techniques (such as FACS sorting) that relies on a distinct separation between a positive and negative population.

Several solutions to these individual problems have been suggested. For example the use of T7 polymerase to amplify Riboswitch output and improve the functional range of a riboswitch [27] or to use self-cleaving Ribozymes allowing for greater flexibility in aptamer domain selection[28]. However T7 polymerase relies on a low basal expression limiting it application and ribozymes are a limited in the relatively small number of novel ribozyme catalysts [29].

To overcome the limitations of large 5' fusions, narrow induction range and sensitivity to ORF changes of both engineered and natural riboswitches, we designed and tested Ribo-attenuators (ATTs). These novel genetic elements are placed 150 base pairs into the ORF that the riboswitch is reported to express. They consist of an RBS with an engineered hairpin followed by a negative one shifted transcriptionally fused stop and start codon (TAATG) (figure 2). Translation from this second RBS independent of the riboswitch is silenced through the engineered hairpin over the RBS core. Passage of ribosomes recruited by the

upstream riboswitch then open up the introduced hairpin before dissociating at the proximal in frame stop codon (TAA) in the transcriptionally-fused junction. Further ribosomes can then assemble at the second RBS and initiate translation at the first start codon of the introduced gene of interest. In this fashion instead of directly controlling the translation of a gene as in its natural setting, the riboswitch instead controls the translational initiation rate from the downstream attenuator RBS. As such Ribo-attenuators allow for the fine tuning of a riboswitch response, the orthogonal expression of a novel gene of interest and by improving the reliability with which the downstream RBS remains exposed, they also reduce variation within populations. Ribo-attenuators overcome the main issues preventing the wide spread use of re-engineered or synthetic riboswitches.

Materials and methods

Plasmids

All riboswitch cassettes were cloned into the J64100 plasmid[30] (ColE1 origin; 50-60 copies, Chloramphenicol resistance) under control of the tetracycline promoter. The Adda riboswitch sequence was the kind donation from Dr Neil Dixon (Department of Chemistry, University of Manchester) and the Btub riboswitch was taken from the *Escherichia coli* genome. All riboswitches were synthesised by IDT (Skokie, IL, USA) as gBlock gene fragments, assembled by Gibson assembly [31,32] and sequence confirmed. A full list of plasmids, GeneBank accession numbers and Addgene references are available in Table 1. A full list of Ribo-attenuator sequences is available in table 2.

Growth and induction

All experiments were performed in *E. coli* DH5alphaZ1 [33]. For each experiment three freshly transformed colonies were inoculated in LB medium (10g/L tryptone, 5g/L yeast extract, 10g/L NaCl) with chloramphenicol (25µ/mL) and grown overnight then diluted 1:100 into 1 mL LB in a deep well plate (Greiner bio-one) with chloramphenicol (25 µ/mL),

Anhydrotetracycline (150 ng/mL) and stated concentrations of riboswitch inducer. Cultures were induced for 8 hours at 37 °C with shaking before data collection. Biological triplicates were chosen to ensure adequate analysis of the standard deviation around the mean.

Data measurements

After induction 200 µL of each culture was centrifuged at 4000 RPM, washed with PBS and resuspended in 500 µL of PBS. OD_{600} measurements were taken in clear well plates and GFP measurements in black well plates in a clariostar platereader (BMG Labtech, Ortenberg, Germany). GFP was quantified by normalising by OD_{600}. Flow cytometry was performed on an Attune flow cytometer (Lifetech Scientific, Basingstoke, UK) for each data point and 50,000 events were measured.

Fluorescence microscopy

Fluorescence microscopy was performed on cells grown and induced as described above. Thin, flat agarose pads (1% agarose in Milli-Q water, w/v) were generated on microscope slides. Two microliters of cells were added to the pad immobilising them on the surface of the agarose. Cells were then imaged with a Nikon Eclipse Ti microscope, 100X phase contrast objective (Nikon), GFP filter set (Chroma), Andor iXON CCD camera. Images were acquired using NIS Elements software (Nikon).

Model Methods

The cumulative distribution of the random variable T denoting the time elapsed between an arbitrary time-point T and the next production of a GFP molecule was calculated according to the model described in the Supplementary Information. We used the following parameter values.

$$\lambda(\mathrm{ON}) = 50, \mu(\mathrm{ON}) = 4, \lambda(\mathrm{OFF}) = \mu(OFF) = 0.01 K\_ = 0.5 m\_ = 1)$$

$$K_{+(I)} = \frac{(I)^2}{(I)^2 + 10^2}$$

For $0 \leq [I] \leq 50$ (where $[I] = 50$ corresponds to 100% induction). The inverse of T is the random variable we call "Expression Rate". For the calculation of the CDFs, see Supplementary Information and the corresponding MATLAB code.

Results

Change in open reading frame demonstrate sensitivity of 5' regulatory elements to secondary structure.

Two previously reported riboswitches were investigated for sensitivity to changes in ORF. An Adda riboswitch characterised from *Vibrio vulnificus* [15,34] is an activating purine riboswitch [35–37]. It is reported to selectively bind 2-aminopurine. Fusing SFGFP to the first 150 base pairs of the previously reported ORF [15] yielded an induction response very similar to previously reported studies between 0 and 250 µM 2-aminopurine. However, directly replacing the reported ORF with SFGFP (start codon for start codon) gave no induction response. These data were supported by single cell analysis showing that when a fusion was used the population responded to the inducer. However when the ORF was completely substituted no such response was seen (figure 3A).

The Btub riboswitch is a repressive riboswitch that responds to adenosylcobalamin, an active form of vitamin B_{12} [38] and represents a riboswitch responding to a high value small metabolite. As with the Adda riboswitch, fusion of GFP to 150 base pairs of the working ORF yielded a repressive induction response between 0 and 50 nM of adenosylcobalamin. Replacing the working ORF with GFP (start codon for start codon) resulted in a loss of this induction response. Analysis of the single cell data also showed no response to the presence of adenosylcobalamin when the ORF was completely replaced (figure 3B).

Design of Ribo-attenuators.

To test the hypothesis that a RNA attenuator could overcome some of the underlying difficulties surrounding riboswitches, we added a second RBS downstream of the riboswitch. The RBS used was SD1 taken from the BIOFAB parts library [39] and adapted to have a negative one base shifted start codon (TAATG). Translation from this RBS independent of the riboswitch was silenced by secondary structure introduced around the RBS by an engineered hairpin. To design the attenuators we first expressed the RBS alone from the tetracycline promoter. We then introduced engineered hairpins with an ever lower ΔG over the RBS on the 5' end. One attenuator had the hairpin in the 3' side. These new RBS showed a significant drop in translational efficiency with the exception of the smallest hairpin (Supplementary figure S1). Screening of hairpins of N+3 bp from 3-24 bp stem loop yielded a step like expression profile with a step function happening every 6 bp. Ribo-attenuators were chosen as the least variable candidate in each plateau. Further Ribo-attenuators could easily be designed rationally around a new RBS using these design principles or using random primer bases followed by a screen for the Ribo-attenuator of required strength. Care was taken that the stop codon in the translational fusion between the Ribo-attenuator and the gene of interest was introduced to be in frame with any ribosome that came from the riboswitch.

Ribo-attenuators allow Adda riboswitch re-engineering for a ~14.5 fold dynamic activation range.

Five Ribo-attenuators were introduced to the adenine riboswitch 150 base pairs after the riboswitch ATG. This yielded a dynamic response of ~14.5 fold between the lowest and highest attenuator (figure 4A) .The induction profile was closely associated with the strength of the attenuator in a predictable fashion i.e. stronger hairpin leads to a narrower and lower induction response. The fusion of SFGFP to the working ORF yielded very clear inclusion

bodies (Figure 4B). These are shown as distinct spots present at one pole of the cell and are formed by misfolded insoluble proteins. By comparison the attenuated riboswitch (att1 shown) yielded soluble protein as the translated reporter gene is expressed orthogonally from the upstream 150 base pairs or working ORF. Full single cell data is shown in Supplementary figure S2

Ribo-attenuators allow Btub riboswitch re-engineering for a ~18.5 fold dynamic activation range.

The same five Ribo-attenuators were introduced to the Btub riboswitch after 150 bp of the working ORF. This yielded a dynamic response of ~18.5 fold between the lowest and highest attenuator. As with the Adda riboswitch, increased secondary structure tuned down expression with the Ribo-attenuators all displaying a similar response (Figure 5A). Introduction of the attenuators allowed for a notable difference between an activated and an unactivated riboswitch as shown by fluorescence microscopy (Figure 5B). Full single cell data is shown in Supplementary figure S2.

Ribo-attenuators reduce uncertainty of riboswitch function

The translation of GFP from mRNA in the one-component system at any given time depends on the position of the riboswitch, either lambda_ON or lambda_OFF. Over time the riboswitch stochastically switches between ON and OFF, with the inducer concentration biasing the stochastic switching towards one or the other state. Assuming that the two translation rates are at different orders of magnitude, the waiting time from any given time until the production of a GFP molecule is thus highly uncertain.

In the two-component case (with the addition of a ribo-attenuator), the two switches can be in one of four states (OFF, OFF), (OFF, ON), (ON, OFF), and (ON, ON). The rates lambda_ON and lambda_OFF of ribosome transit are now the rates at which the second switch turns on, given the state of the first. The scale separation of those rates means that,

to a first approximation, the first switch ON implies the second switch will turn ON, and the first switch OFF implies the second switch is likely to turn OFF. However, the GFP translation rates μ_ON and μ_OFF resulting from the state of the second switch can now be set independently of the translation parameters of the upstream riboswitch. This is due to the introduction of the secondary RBS in the Ribo-attenuator that can be modulated.

Figure 6(A) displays a schematic of this model; the length of the attenuator region determines the frequency at which the attenuator region switches off. Figure 6(B) plots the probability distribution at maximal induction of the total number of GFP molecules produced in a given unit time interval for our stochastic model, for the riboswitch fusion and the Ribo-attenuator in blue and red respectively. The distribution of the Ribo-attenuator system is clearly tighter around its mean, reflecting a reduction in the uncertainty of gene expression over time. Figure 6(C) shows the mean and standard deviations of these two distributions as the inducer concentration increases from 0% to 100% induction. The results of our modelling suggest an approximately 30% reduction in standard deviation for the Ribo-attenuator system across most induction strengths, compared to the riboswitch fusion. The plots in figure 6(D) show an overlay between the Adda and Btub riboswitches and a similarly expressing attenuator. This experimental evidence for a reduction in unpredictability in GFP expression, which we assume to be the direct consequence of uncertainty in GFP translation initiation rates. Figure 6(E) displays the single cell distinction between uninduced and fully induced populations showing that variation was reduced within populations as shown by the narrowing of the flow cytometry population data. The overlapping populations with the fusion are made much more distinct with the addition of the Ribo-attenuator. Similar overlay for the Btub riboswitch was observed and is shown in supplementary figure 3. The one-component system has an extremely uncertain distribution of translation rates in comparison to the two-component system.

Discussion

We designed a novel and widely applicable tool that allows riboswitches to be used as modular, tunable components with a highly predictable outcome, enhancing applicability by overcoming previously identified drawbacks. We chose two well known, representative riboswitches; the Adda riboswitch, an activating class of riboswitches that respond to a cellular metabolite (Adenine) and the Btub riboswitch which responds to adenosylcobalamin. These have the potential to facilitate the biological production of high value micronutrients, for example vitamins, many of which are still produced by expensive and inefficient chemical synthesis. Recently described methods applying riboswitches against high value vitamins could be used with the ribo-attenuators described here to elicit a high throughput approach of pathway elucidation[40].

The first step towards improving the applicability of a riboswitch is facilitating the independent translation of a new ORF to suit a novel purpose. This new ORF should be translated independent of any fusion domain. A previously reported riboswitch would be adapted as a reporter for a high value chemical or to control a downstream process by expressing a replaced gene. In a traditional transcription factor controlled biosensor, this would be achieved by substituting the original ORF with a new one on a 'start codon for start codon' basis. However some riboswitches have been reported to be sensitive to these changes[20], with their aptamer domain extending into their ORF or in other ways sensitive to changes in secondary structure in this region. A typical solution is to fuse the new gene of interest to the first 150 base pairs of the working ORF [38,41–43]. Re-engineering a riboswitch to express a reporter gene in this fashion gives rise to a protein with a large fusion which could severely impact function. Replacing the reported ORF completely often results in a change of context and a complete loss of response. If a fusion as in figure 3 had been taken to express a new enzyme potential inclusion bodies would have severe limitations to its usefulness. We hypothesise these inclusion bodies are present because the working ORF contains a beta strand which when expressed as a fusion causes the resulting protein to have an uneven number of beta strands and thus mis-fold.

Ribo-attenuators allow for a new ORF to be independently translated from any 5' region thanks to independent ribosome initiation from RBS2.

The second step towards applicability is changing the induction response of a riboswitch to its inducer. While some studies focus on boosting riboswitch efficiency through RNA amplification [27] and others focus on the *de-novo* design of synthetic riboswitches [19], none provide a reliable, modular and predictable approach to changing the induction range of a riboswitch for a different application. Ribo-attenuators allow for a predictable approach to changing riboswitch induction response. This tuning centres around binding of the ribosome around the Ribo-attenuator RBS and interference of this by the formation of the introduced hairpin. This reassembly around the attenuator can be fine-tuned through easily predicted secondary structure and RBS translation initiation rate whilst preserving the riboswitch response.

A third limitation to the application of riboswitches is the unpredictability of their output. This restricts the application of riboswitches in two ways; an unpredictable population is very hard to separate by FACS. This limits the ability for library screening for a novel compound; secondly a widely distributed population can produce downstream variance in the process the riboswitch controls. Both are issues for the application of many riboswitches. We modelled the system in order to explain the distinct populations that came from the use of Ribo-attenuators. Our model demonstrates that the introduction of Ribo-regulators has a small effect on reducing the mean expression rates, but a very large effect in reducing the variability in stochastic expression rates. Furthermore, Ribo-regulators differ significantly from other attempts at riboswitch re-engineering in that the expression rate μ_{ON} is easily and predictably changed.

In conclusion using the Ribo-attenuators' dynamic response to fine tune sensitivity combined with the low uncertainty and more distinct separation of populations, riboswitches could be more readily used in many applications such as FACS screening of a library for rapid pathway elucidation for a potential novel biosynthesis pathway. Initially we examined the sensitivity of two well-known riboswitches to the introduction of a new open reading frame, the fusion of the novel reporter yielding functional riboswitches but in one case inclusion bodies significantly limits application. We also observed a high degree of variation in the Adda riboswitch which made identification of specific concentrations of ligand very difficult. By the use of Ribo-attenuators we allowed both riboswitches to maintain the original open reading frame and as a result ligand response, while expressing the gene of interest orthogonally over a predictable dynamic range. Using these Ribo-regulators it should be possible to overcome limitations identified in previous studies for example the Glycine riboswitch is a similar riboswitch from *Bacillus subtilis* identified as having a narrow 6 fold induction range [44]. Its potential use as a tool maintaining vectors in the absence of an antibiotic or the cheap induction in a bioreactor through Glycine induction is limited by its narrow and fixed induction range. As shown in figure 5 for the Btub riboswitch, ribo-attenuators could improve the small six fold static response to one where this riboswitch could fulfil one of these roles above. The reduction in noise could also facilitate riboswitch application: using the Ribo-attenuators to control expression of a re-constituted gene could yield a more homogeneous expression profile and could facilitate more accurate library selection. In summary, Ribo-attenuators represent a breakthrough step towards allowing riboswitches to be treated as truly modular devices in a plug and play system.

Acknowledgments

Drew Endy, George Wadhams, Chris Grant, Ciarán L Kelly, Karl brune, Axel nystrom. Members of the Bayer and Papachristodoulou groups.

Funding

Support for this work came from the EPSRC project EP/M002454/1. and the BBSRC project BB/L002507/1

Author contributions

TF, TB, JPA and LJR designed the research, TF and CWJ performed experiments, TPP and AP did modelling and computational work. All authors analysed data and wrote the paper.

Competing financial interests

The authors declare no competing financial interests

References

1. Serganov, A. & Patel, D. J. Ribozymes, riboswitches and beyond: regulation of gene expression without proteins. *Nat. Rev. Genet.* **8,** 776–790 (2007).

2. Breaker, R. R. Riboswitches and the RNA world. *Cold Spring Harb. Perspect. Biol.* **4,** (2012).

3. Groisman, E. A., Cromie, M. J., Shi, Y. & Latifi, T. A Mg2+-responding RNA that controls the expression of a Mg2+ transporter. *Cold Spring Harb. Symp. Quant. Biol.* **71,** 251–8 (2006).

4. Mandal, M. & Breaker, R. R. Adenine riboswitches and gene activation by disruption of a transcription terminator. *Nat. Struct. Mol. Biol.* **11,** 29–35 (2004).

5. Serganov, A., Huang, L. & Patel, D. J. Structural insights into amino acid binding and gene control by a lysine riboswitch. *Nature* **455,** 1263–1267 (2008).

6. Wacker, A. *et al.* Structure and dynamics of the deoxyguanosine-sensing riboswitch studied by NMR-spectroscopy. *Nucleic Acids Res.* **39,** 6802–6812 (2011).

7. Li, S. & Breaker, R. R. Eukaryotic TPP riboswitch regulation of alternative splicing involving long-distance base pairing. *Nucleic Acids Res.* **41,** 3022–31 (2013).

8. Rinaldi, A. J., Lund, P. E., Blanco, M. R. & Walter, N. G. The Shine-Dalgarno sequence of riboswitch-regulated single mRNAs show ligand-dependent accessibility bursts. *Nat. Commun.* **7,** 1–10 (2016).

9. Reining, A. *et al.* Three-state mechanism couples ligand and temperature sensing in riboswitches. *Nature* **499,** 355–359 (2013).

10. Chen, Y. Y., Galloway, K. E. & Smolke, C. D. Synthetic biology: advancing biological frontiers by building synthetic systems. *Genome Biol.* **13,** 240 (2012).

11. Isaacs, F. J. *et al.* Engineered riboregulators enable post-transcriptional control of gene expression. *Nat. Biotechnol.* **22,** 841–7 (2004).

12. Rodrigo, G. *et al.* Full Design Automation of Multi-State RNA Devices to Program Gene Expression Using Energy-Based Optimization. *PLoS Comput. Biol.* **9,** e1003172 (2013).

13. Wittmann, A. *et al.* Selection of tetracycline inducible self-cleaving ribozymes as synthetic devices for gene regulation in yeast. *Mol. Biosyst.* **7,** 2419 (2011).

14. Wieland, M. & Hartig, J. S. Artificial Riboswitches: Synthetic mRNA-Based Regulators of Gene Expression. *ChemBioChem* **9,** 1873–1878 (2008).

15. Dixon, N. *et al.* Reengineering orthogonally selective riboswitches. *Proc. Natl. Acad. Sci. U. S. A.* **107,** 2830–5 (2010).

16. Lin, Y.-H. & Chang, K.-Y. Rational design of a synthetic mammalian riboswitch as a ligand-responsive -1 ribosomal frame-shifting stimulator. *Nucleic Acids Res*. (2016). doi:10.1093/nar/gkw718

17. Wachsmuth, M., Findeiß, S., Weissheimer, N., Stadler, P. F. & Mörl, M. De novo design of a synthetic riboswitch that regulates transcription termination. *Nucleic Acids Res*. **41,** 2541–51 (2013).

18. Beisel, C. L. & Smolke, C. D. Design Principles for Riboswitch Function. *PLoS Comput. Biol.* **5,** e1000363 (2009).

19. Espah Borujeni, A., Mishler, D. M., Wang, J., Huso, W. & Salis, H. M. Automated physics-based design of synthetic riboswitches from diverse RNA aptamers. *Nucleic Acids Res*. **44,** 1–13 (2016).

20. Caron, M.-P. *et al.* Dual-acting riboswitch control of translation initiation and mRNA decay. *Proc. Natl. Acad. Sci. U. S. A.* **109,** E3444–53 (2012).

21. Renzi, F. *et al.* Large-scale purification and crystallization of the endoribonuclease XendoU: troubleshooting with His-tagged proteins. *Acta Crystallogr. Sect. F. Struct. Biol. Cryst. Commun.* **62,** 298–301 (2006).

22. Amor-Mahjoub, M., Suppini, J.-P., Gomez-Vrielyunck, N. & Ladjimi, M. The effect of the hexahistidine-tag in the oligomerization of HSC70 constructs. *J. Chromatogr. B* **844,** 328–334 (2006).

23. Chant, A., Kraemer-Pecore, C. M., Watkin, R. & Kneale, G. G. Attachment of a histidine tag to the minimal zinc finger protein of the Aspergillus nidulans gene regulatory protein AreA causes a conformational change at the DNA-binding site.

Protein Expr. Purif. **39,** 152–159 (2005).

24. Woestenenk, E. A., Hammarström, M., van den Berg, S., Härd, T. & Berglund, H. His tag effect on solubility of human proteins produced in Escherichia coli: a comparison between four expression vectors. *J. Struct. Funct. Genomics* **5,** 217–29 (2004).

25. Wu, J. & Filutowicz, M. Hexahistidine (His6)-tag dependent protein dimerization: a cautionary tale. *Acta Biochim. Pol.* **46,** 591–9 (1999).

26. Horchani, H., Ouertani, S., Gargouri, Y. & Sayari, A. The N-terminal His-tag and the recombination process affect the biochemical properties of Staphylococcus aureus lipase produced in Escherichia coli. *J. Mol. Catal. B Enzym.* **61,** 194–201 (2009).

27. Emadpour, M., Karcher, D. & Bock, R. Boosting riboswitch efficiency by RNA amplification. *Nucleic Acids Res.* **43,** e66–e66 (2015).

28. Felletti, M., Stifel, J., Wurmthaler, L. A., Geiger, S. & Hartig, J. S. Twister ribozymes as highly versatile expression platforms for artificial riboswitches. *Nat. Commun.* **7,** 12834 (2016).

29. Franzen, S. Expanding the catalytic repertoire of ribozymes and deoxyribozymes beyond RNA substrates. *Curr. Opin. Mol. Ther.* **12,** 223—232 (2010).

30. Bonnet, J., Yin, P., Ortiz, M. E., Subsoontorn, P. & Endy, D. Amplifying genetic logic gates. *Science* **340,** 599–603 (2013).

31. Gibson, D. G. *et al.* Enzymatic assembly of DNA molecules up to several hundred kilobases. *Nat. Methods* **6,** 343–5 (2009).

32. Gibson, D. G. *et al.* Creation of a bacterial cell controlled by a chemically synthesized genome. *Science (80-.).* **329,** 52–56 (2010).

33. Lutz, R. & Bujard, H. Independent and tight regulation of transcriptional units in Escherichia coli via the LacR/O, the TetR/O and AraC/I1-I2 regulatory elements. *Nucleic Acids Res.* **25,** 1203–10 (1997).

34. Serganov, A. *et al.* Structural basis for discriminative regulation of gene expression by adenine- and guanine-sensing mRNAs. *Chem. Biol.* **11,** 1729–41 (2004).

35. Gong, S., Wang, Y. & Zhang, W. Kinetic regulation mechanism of pbuE riboswitch. *J. Chem. Phys.* **142,** 015103 (2015).

36. Rieder, R., Lang, K., Graber, D. & Micura, R. Ligand-Induced Folding of the Adenosine Deaminase A-Riboswitch and Implications on Riboswitch Translational Control. *ChemBioChem* **8,** 896–902 (2007).

37. GILBERT, S. D., MONTANGE, R. K., STODDARD, C. D. & BATEY, R. T. Structural Studies of the Purine and SAM Binding Riboswitches. *Cold Spring Harb. Symp. Quant. Biol.* **71,** 259–268 (2006).

38. Franklund, C. V & Kadner, R. J. Multiple transcribed elements control expression of the Escherichia coli btuB gene. *J. Bacteriol.* **179,** 4039–42 (1997).

39. Mutalik, V. K. *et al.* Precise and reliable gene expression via standard transcription and translation initiation elements. *Nat. Methods* **10,** 354–360 (2013).

40. Zhu, X., Wang, X., Zhang, C., Wang, X. & Gu, Q. A riboswitch sensor to determine vitamin B12 in fermented foods. *Food Chem.* **175,** 523–8 (2015).

41. Nou, X. & Kadner, R. J. Coupled changes in translation and transcription during cobalamin-dependent regulation of btuB expression in Escherichia coli. *J. Bacteriol.* **180,** 6719–28 (1998).

42. Winkler, W., Nahvi, A. & Breaker, R. R. Thiamine derivatives bind messenger RNAs directly to regulate bacterial gene expression. *Nature* **419,** 952–6 (2002).

43. Dixon, N. *et al.* Orthogonal riboswitches for tuneable coexpression in bacteria. *Angew. Chem. Int. Ed. Engl.* **51,** 3620–4 (2012).

44. Phan, T. T. P. & Schumann, W. Development of a glycine-inducible expression system for Bacillus subtilis. *J. Biotechnol.* **128,** 486–499 (2007).

Figure legends:

Table 1:List of strains, plasmids and Genbank references. All plasmids were submitted to Addgene.

Table 2:List of Ribo-attenuator sequences.

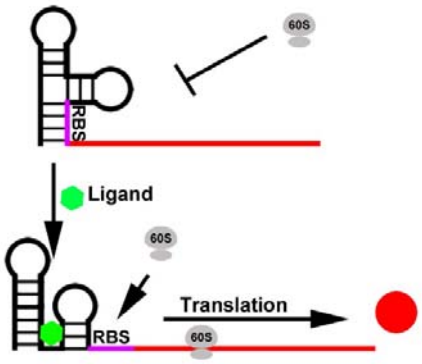

Figure 1: **Typical riboswitch function:** An RBS (purple) is sequestered away within a riboswitch preventing ribosome recruitment, binding of a ligand (green) causes a

conformational change exposing the RBS, allowing for translation of the gene of interest (red).

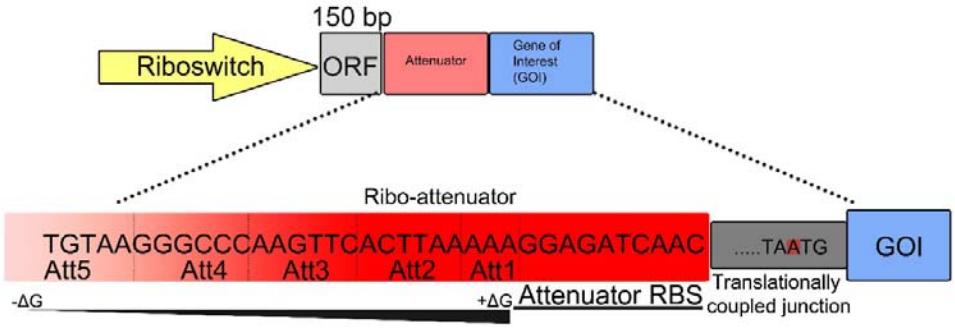

Figure 2: **Ribo-attenuator Context and schematic**: We defined a Ribo-attenuator element to describe the boundaries and genetic elements that compose a Ribo-attenuator and set this within relevant genetic context. The Ribo-attenuator is situated after the riboswitch and 150 bps of its accompanying ORF. Each Ribo-attenuator consists of an RBS and a translationally coupled junction, Att1 started with a short 3 base pair hairpin with a high delta G, further ribo-attenuators had a larger hairpin and lower delta G.

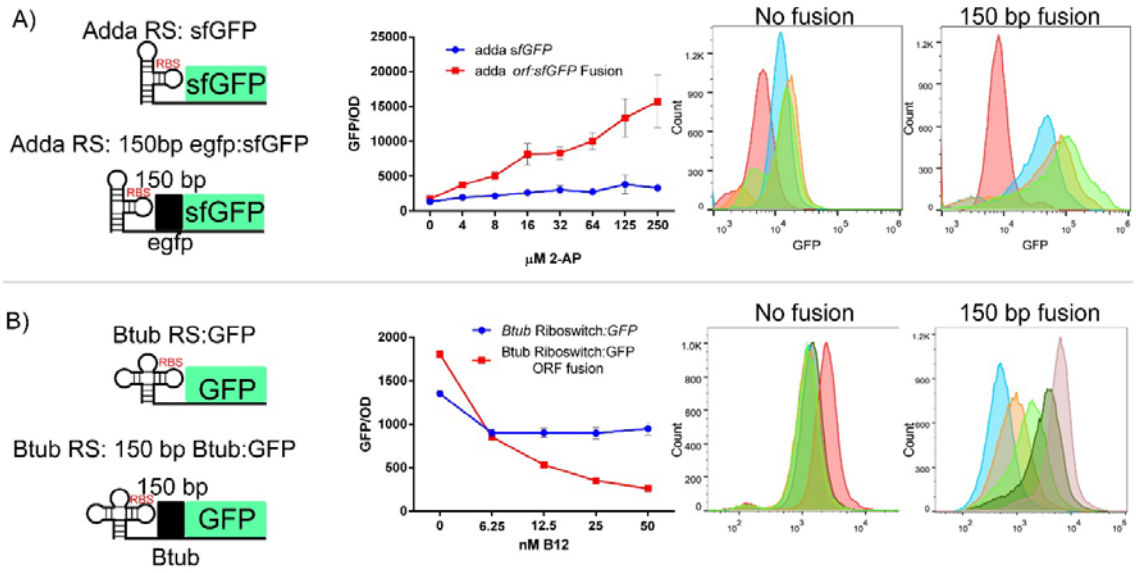

Figure 3: **Adda and Btub riboswitches exhibit contextual sensitivity**: (A) The Adenine riboswitch had SFGFP Introduced directly after the riboswitch replacing it's reported ORF and fused to the first 150 bps of the reported ORF. Both constructs were analysed for population and single cell response to 2-aminopurine.Error bars indicate standard deviation around the mean for biological triplicates. Single cell colours; Red (0 μM) Blue (8μM) Orange (32μM) Green (250μM). (B) The Btub riboswitch had eGFP introduced directly after the reported ORF and fused to the first 150 bps of the reported ORF. both constructs were analysed for population and single cell response to adenosylcobalamin. Single cell colours; Red (0 nM) Dark green (6.25 nM) Light green(12.5nM) Orange (25nM) Blue (50 nm).

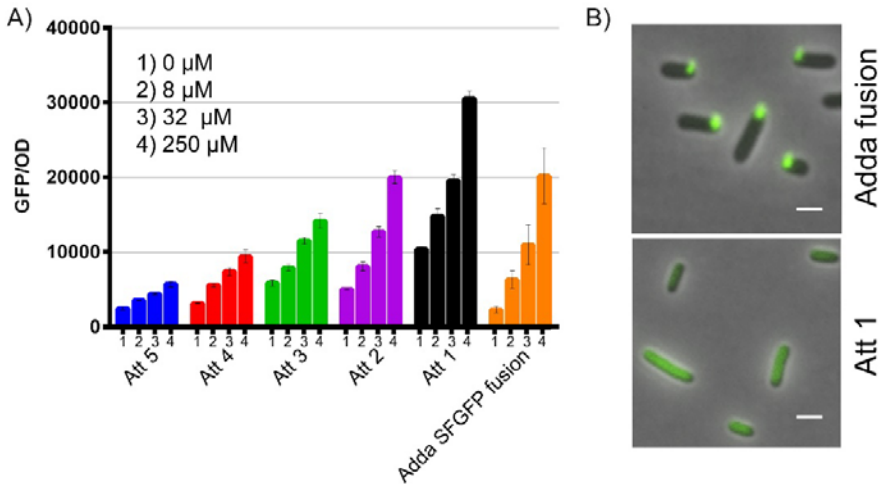

Figure 4: **Ribo-attenuators allow Adda riboswitch rational re-engineering** (A) Response of each Ribo-attenuator to 0, 8, 32 and 250 µM 2-aminopurine as compared to the fusion construct (orange bars) Error bars indicate standard deviation around the mean for biological triplicates . Full single cell data is shown in supplementary figure 2. (B) Fluorescence microscopy of the Adda fusion showing clear inclusion bodies and the Att1 Ribo-attenuator showing soluble dispersed GFP. White bars represent 1µm.

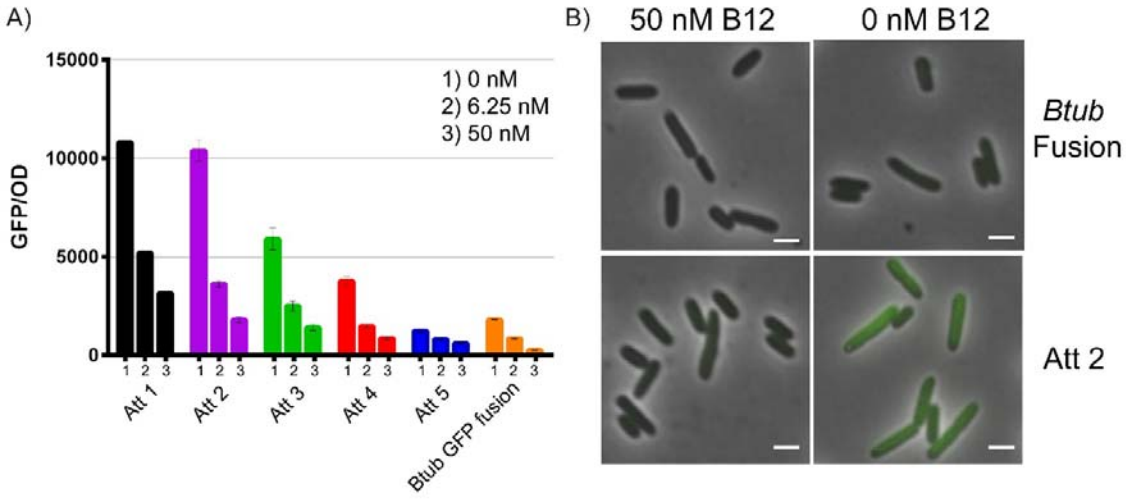

Figure 5: **Ribo-attenuators allow Btub riboswitch rational re-engineering** (A) Response of each Ribo-attenuator to 0, 8, 32 and 250 μM 2-aminopurine as compared to the fusion construct (orange bars) Error bars indicate standard deviation around the mean for biological triplicates. Full single cell data is shown in supplementary figure 2. (B) Fluorescence microscopy of the uninduced and induced Btub fusion and Att2 ribo-attenuated Btub riboswitch showing a clearer induction difference. White bars represent 1μm.

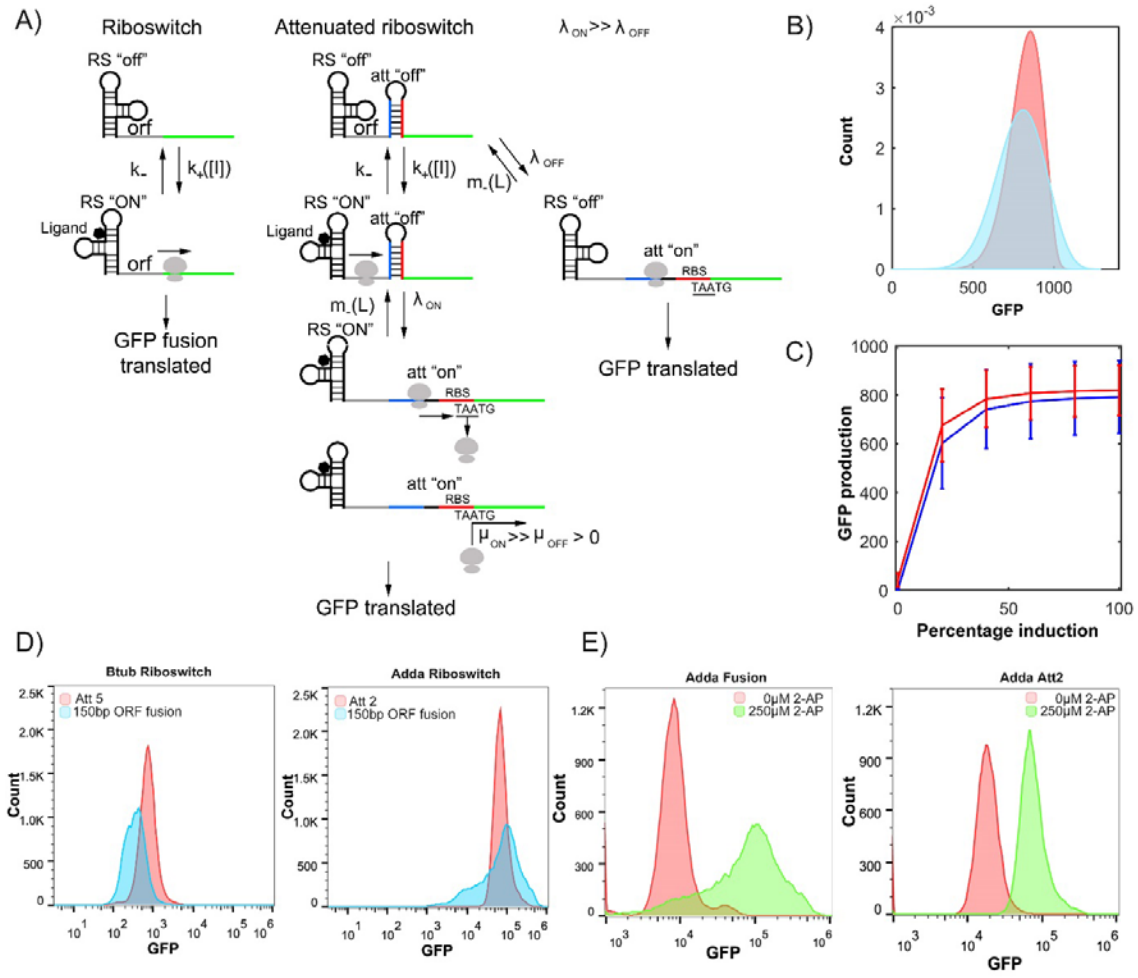

Figure 6: **Ribo-attenuators reduce riboswitch noise** (A) Random walk dynamics. The riboswitch of the one-component system randomly switches between OFF and ON states at rates k_+([I]) and k_-, where k_+ is an increasing function of inducer concentration. GFP is produced at rate λ{OFF} or λ{ON} depending on the state of the riboswitch. In the two-component system, the riboswitch has similar dynamics; the rates λ {OFF} and λ {ON} are now the rates at which the downstream attenuator is switched ON. The downstream attenuator can spontaneously switch off at rate m_-(L), which is an increasing function of the length L of the attenuator region. GFP is produced at rates μ{OFF} and μ {ON} depending on the state of the downstream attenuator. (B) Probability distribution for the random variable defined as the number

of GFP molecules expressed by the stochastic model in (A) over a unit time interval starting from arbitrary (long-term) time-point, for a given "full" induction strength. The blue curve shows the probability distribution for the riboswitch fusion system, and the red curve shows the probability distribution for the attenuated riboswitch. (C) The mean (main curve) plus/minus one standard deviation (error bars) of the probability distribution of the random variable described above, for varying induction concentrations defined as a percentage of "full" induction. The blue curve shows the means and standard deviations for the riboswitch fusion system, and the red curve shows the means and standard deviations for the attenuated riboswitch. See Materials & Methods for parameters used to produce (B) and (C). (D) Overlay of the Btub riboswitch with a functional fusion (blue) and with att5 (red), and overlay of the Adda riboswitch with a functional fusion (blue) and Att2 (red). (E) Single cell distinction between the lower and upper limits of the Adda riboswitch fused to GFP and with the Att2 Ribo-attenuator showing more distinct populations with the addition of the Ribo-attenuator.